ACS Macro Letters

Letter

pubs.acs.org/macroletters

Polymer Microstructures Self-Assemble on Single-Walled Carbon Nanotube Thin Films

Zhenquan Tan* and Hiroya Abe

Joining and Welding Research Institute, Osaka University, 11-1 Mihogaoka, Ibaraki, Osaka 567-0047, Japan

Supporting Information

ABSTRACT: The formation of self-assembled microstructures of anionic polyelectrolyte, poly(acrylic acid) salts, on the surface of single-walled carbon nanotube thin films was studied by a fast phase separation process that filtrated a mixed dispersion composed of single-walled carbon nanotubes and poly(acrylic acid) derivatives on a membrane filter. The resulting microstructures of poly(acrylic acid) self-assembly were characterized by scanning electron microscopy, energy-dispersive X-ray spectroscopy, element mapping, and diffuse reflectance Fourier transform infrared spectroscopy. The influence factors including substrate, ion species, single-walled carbon nanotubes, and different kinds of carbon nanotubes were discussed comprehensively for the formation of microstructures of PAA self-assembly by a liquid−liquid phase separation.

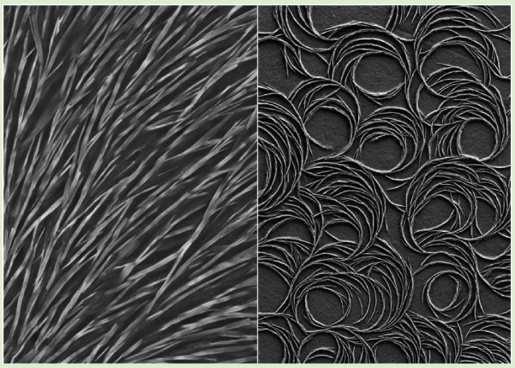

Composite materials composed of single-walled carbon nanotubes (SWCNTs) and polymers, which possess many attractive mechanical, electronic, and chemical properties, have received tremendous attention due to their wide applications in the fields ranging from reinforcement, superhydrophobic surface to sensors, light-emitting diode display, and biological applications.[1−6] Crystallization and phase separation are common phase behaviors in polymers and generally considered a big problem that must be prevented in the formation of polymer−SWCNT composites.[7] However, by making good use of the phase separation of polymers, some previous researches also reported the design to construct periodic functionalized patterning on carbon nanotubes,[8−10] which suggests a facile approach for the synthesis of unique SWCNT-based heterogeneous nanostructures.

Phase separation is widely observed in various kinds of condensed matter including metals, semiconductors, polymers, and biological materials and plays key roles in the physiochemical processes ranging from crystal nucleation, protein purification, to petroleum refining.[11−14] Phase separation provides an effective and controllable approach to synthesize fine-defined nanostructures with well-designed morphology such as quantum dots, nanostructures, and photonic materials.[15−20] Wendlandt reported that the symmetric boundary of the substrate played important roles in the phase separation of polymer blend in thin films.[21] A designedly patterned substrate was used to control the final nanostructures of polymer from phase separation.[22] However, very few studies were addressed on phase separation in a composite system composed of polymers and SWCNTs. It is useful to study the phase separation and nanostructure formation of polymers on a special boundary, SWCNT thin films.

Here we report a phase separation in which poly(acrylic acid) (PAA) forms self-assembled microstructures on SWCNT thin films by filtration of a mixed suspension containing PAA and SWCNTs. PAA and its derivatives are one kind of anionic polyelectrolyte and have been widely used as dispersing, suspending, and emulsifying agents in pharmaceuticals and cosmetics.[23]

Some previous researches have reported the phase separation behavior of PAA and its derivatives.[24−26] In our study, PAA derivatives formed ordered self-assembled microstructures on the designed boundary (SWCNT thin films) from phase separation induced by metal ions in the presence of surfactants. The existence of metal ions as a cosolute greatly affected the phase separation behavior of polymer by preventing or promoting the phase separation.[27−29] The effect of metal ion species was investigated in the phase separation of PAA derivatives in this study. We also investigated the effect of surfactants and temperature for the final morphology of PAA self-assembly achieved from phase separation. Some beautiful artistic patterns were obtained by carefully selecting the conditions of phase separation. This study may improve our knowledge on the phase separation behavior of PAA derivatives.

The experimental details are demonstrated in the Supporting Information. When the mixed aqueous dispersion composed of SWCNTs and PAA derivatives was filtrated by a membrane filter, SWCNTs were easily deposited on the substrate in comparison with PAA, due to the low viscoelasticity in aqueous dispersion. Hence, SWCNTs first formed a thin film on the

Received: September 27, 2013
Accepted: December 17, 2013
Published: December 19, 2013

   dx.doi.org/10.1021/mz400502v | ACS Macro Lett. 2014, 3, 35−39

membrane filter substrate. Figure 1a demonstrates the deposition and phase separation process of the mixed aqueous

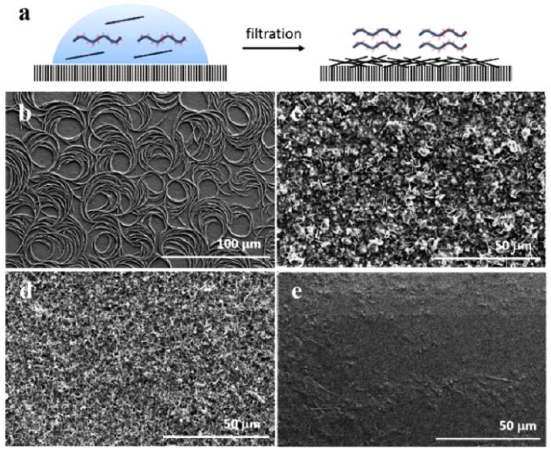

Figure 1. (a) Schematic illustration of deposition and phase separation of mixed aqueous dispersion composed of SWCNT and PAA derivatives. SEM of microstructures of PAA−NH_4 on (b) SWCNT, (c) DWCNT, and (d) MWCNT thin film supported by a VTTP membrane filter and (e) SWCNT thin film supported by fresh mica.

dispersion composed of SWCNTs and PAA on the membrane filter. After formation of the SWCNT thin film, polymer was allowed to deposit on the surface of SWCNT thin film, which resulted in the phase separation of PAA derivatives from aqueous dispersion and the formation of self-assembly microstructures.[29] Figure 1b shows a typical SEM image of microstructures of PAA−NH_4 self-assembly on SWCNT thin film. However, in the case of double-walled (DWCNTs) or multiwalled carbon nanotubes (MWCNTs), PAA−NH_4 did not form any ordered microstructures but only small pieces of microstructures on DWCNT thin film or none of the microstructures on MWCNT thin film. It indicates that the nature of carbon nanotubes indeed affects the phase separation of PAA derivatives. Note that SWCNTs form flat and compact thin films; however, DWCNT thin film is rough and not so compact, and MWCNT thin film is loose and completely incompact (Supporting Information, Figure S1). Hence, the boundary conditions are very different for PAA phase separation with SWCNTs, DWCNTs, and MWCNTs and result in the different microstructures.[21] In addition, when using fresh mica as the substrate, water molecules in the aqueous dispersion only volatilized slowly in the atmosphere, which allowed for a quasi-equilibrium codeposition of SWCNTs and PAA that resulted in a flat and smooth thin film (Figure 1e).

PAA−NH_4 formed self-assembled microstructures on SWCNT thin films. The branches show an approximate distribution sector that the branches symmetrically ramified from the medial part of the mother branch. When the main growth axis changed the angle from 30° to 90° or 180°, a bending multibranched structure (Figure 2a, b) and a ring-type structure (Figure 2c) of PAA were achieved. The bending angle was very sensitive to the formation conditions, and it was still hard to control. Figure 2d shows PAA microstructure that was in blocks with several micrometers and separated from SWCNTs. The cross section of PAA microstructures was about 1 μm × 0.3 μm. As a comparison, SWCNTs were bundled with average diameter of 20 nm. Interestingly, PAA blocks show regular facets, which may be due to the crystalline

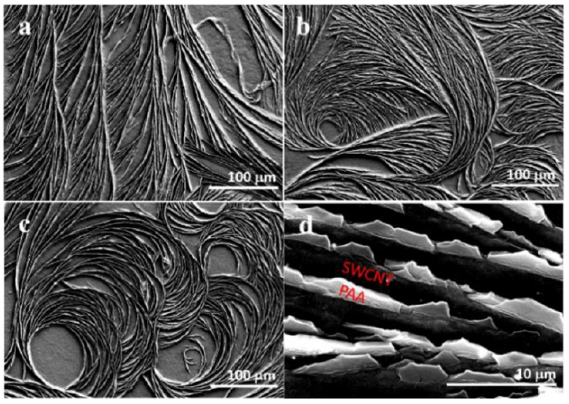

Figure 2. Microstructures of PAA−NH_4 self-assembly with various axial bending angles of (a) 30°, (b) 90°, and (c) 180°. (d) High-resolution SEM photographs of PAA−NH_4 self-assembly.

of PAA generated from dehydration during the filtration process.[30]

Figure 3a shows an energy-dispersive spectroscopy (EDS) pattern of PAA−NH_4 self-assembly on SWCNT thin film.

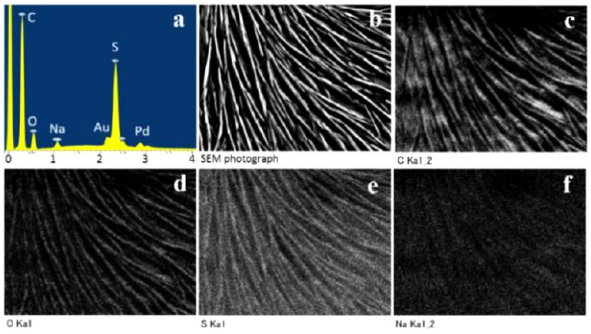

Figure 3. EDS spectroscopy of (a) PAA−NH_4 self-assembly and (b−f) elemental mapping analysis for (c) C, (d) O, (e) S, and (f) Na, respectively.

Several elements were detested by EDS analysis: C, O, S, Na, Au, and Pd. The C signal was contributed from SWCNT, PAA−NH_4, and SDS. The O signal was mainly originated from PAA−NH_4 and sodium dodecyl sulfate (SDS). The S and Na were mainly contributed from SDS. Au and Pd came from the sputtered metals before the EDS measurement. The element distribution in PAA−NH_4 self-assembly was measured by element mapping analysis. Figure 3b shows a SEM photograph that indicated the mapping area. Figure 3c−f shows element distribution of C, O, S, and Na, respectively, accordingly to the SEM photograph. C and O distributions were in good agreement with the SEM photograph. The signals of S and Na were in approximately uniform distribution in the observed area, which suggests that the SDS molecule adsorbed on both the SWCNT and PAA−NH_4 in the mixed dispersion.

FTIR spectroscopy of the as-prepared thin films of SWCNTs and PAA on SWCNTs was displayed in Figure 4. In the sample of SWCNT thin film, the SWCNT showed an infrared absorption at around 1790 cm^{-1}, which was assigned to C=C stretching vibrational features of a graphitic sheet. SDS shows clearly IR absorption in the FTIR spectroscopy.[31] The peaks appearing at 2953, 2904, and 2839 cm^{-1} were assigned to C−H stretching vibrational features of SDS. Two sets of infrared absorption at 1261, 1218 cm^{-1} and 1079, 989 cm^{-1} were

dx.doi.org/10.1021/mz400502v | ACS Macro Lett. 2014, 3, 35−39

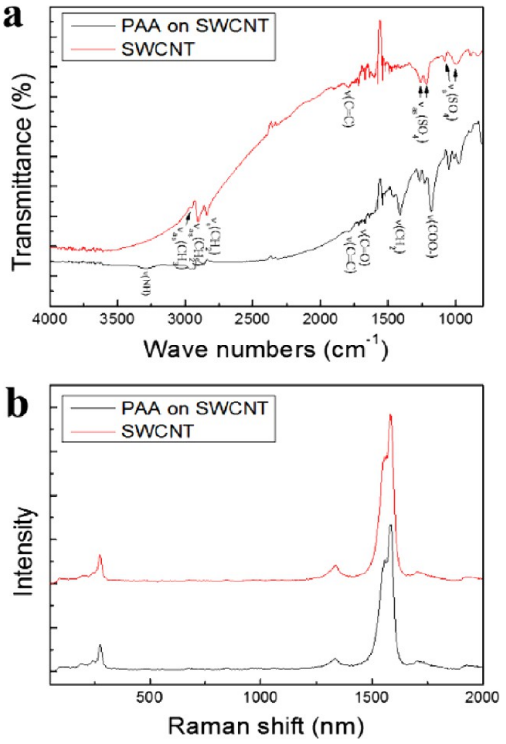

Figure 4. (a) FTIR and (b) Raman spectroscopy of PAA–NH_4 on SWCNT thin film.

originated from the sulfate asymmetric and symmetric stretching bands of SDS, respectively. When PAA–NH_4 phase separated and formed self-assembly on SWCNT thin films, some new, strong IR absorption peaks were observed, which were assigned to the vibrational features of PAA–NH_4. The broad band from 3700 to 2000 cm^{-1} came from the O–H stretching vibration of the carboxylic groups. A weak peak at 3287 cm^{-1} was assigned to N–H stretching vibration of the ammonium salt groups. Two strong peaks at 1411 and 1184 cm^{-1} were assigned to CH_2 scissoring deformation and COOH symmetrical stretching vibrations and deformation.[32] Interestingly, the characteristic peak of C═O stretching vibration at 1715 cm^{-1} was very weak in comparison with previous research.[33] In addition, there was not any new peak observed in Raman spectroscopy after PAA loading (Figure 4b). The Raman shift of the D band and G band of SWCNTs between the two samples has not remarkably changed.

We investigated the phase separation behavior of other PAA derivatives on SWCNT thin film. Figure 5a shows the microstructures of PAA–Na self-assembly from phase separation. PAA–Na formed microstructures that were the same as PAA–NH_4. However, in the case of PAA–H, there was not any ordered microstructure formation (Figure 5b). The surface of the thin film was rough, and many disordered structures were observed. The inset in Figure 5b shows that the disordered structures were aggregates of SWCNTs but not the self-assembly of PAA–H. The difference in phase separation behaviors of PAA derivatives suggests that positive ions in PAA derivatives play critical roles in phase separation, which has been reported elsewhere.[27−29] We added $NH_3{\cdot}H_2O$ or NaOH, respectively, into PAA–H solution in a stoichiometric ratio. It was showed that PAA–H formed ordered microstructures on SWCNT thin film after $NH_3{\cdot}H_2O$ (Figure 5c) or NaOH (Figure 5d) treatment. We also checked the influence of other

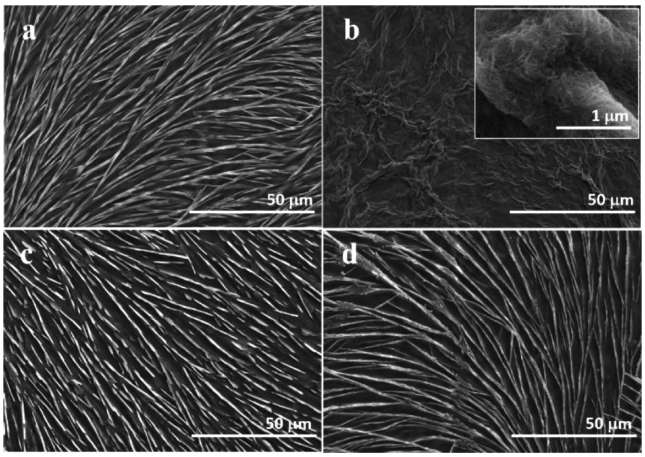

Figure 5. Phase separation of (a) PAA–Na, (b) PAA–H, and PAA–H in the presence of (c) $NH_3{\cdot}H_2O$ or (d) NaOH.

metal ions including Ag^+, Cu^{2+}, and Fe^{3+} (Supporting Information, Figures S2 and S3). All results proved that positive ions promoted the polymer phase separation, which is in good agreement with previous researches.

The phase behavior of PAA derivatives was closely related to the presence of SWCNTs in the mixed dispersion. We found that pure PAA solution resulted in none of the aggregates on the membrane filter in the absence of SWCNTs (Supporting Information, Figure S4). All polymers went through the mesh of the membrane filter. These results suggest that the formation of compact SWCNT thin film is of importance for the phase separation and formation of PAA self-assembly.

Since the formation of the ordered microstructures is closely related to the presence of SWCNTs and positive ions, the formation process is due to the adsorption of PAA on the surface of the SWCNT and the phase behavior of PAA under positive ions surrounding it. Figure 6 demonstrates such a formation process. SWCNTs were dissolved in water assisted with surfactant which adsorbed on the surface of the SWCNT under hydrophobic interaction.[34−36] When the SWCNT met PAA in aqueous dispersion, PAA chains would be attached to the outer surface of surfactant-modified SWCNTs. The chains of PAA were swollen and extended in aqueous dispersion due to the electrostatic repulsion. The extended chains would be rolled up into a spherical conformation induced by the electrostatic attraction between negatively charged polymer chains and positively charged ions.[37] Such PAA-functionalized SWCNTs formed approximate lamella structure by a self-assembly process. On the other hand, pseudospherical micelles may also form in the liquid phase by a liquid–liquid phase separation where SWCNTs are trapped at the liquid–liquid phase boundary,[38,39] which is generated by an emulsion-based process assisted by ultrasonic treatment. During the filtration process, SWCNTs first deposited on the membrane filter substrate, which allows PAA to form parallel-line or ring-type microstructures on SWCNT thin films by a phase separation mechanism.

According to the formation process based on experimental results, we demonstrate that the phase separation is not necessary to be limited in PAA, but it actually happens involving the whole system, in which the SWCNT plays a critical role for the formation of microstructures. To understand the importance of SWCNTs in the process, we perform two controlled experiments to investigate the phase behavior with

dx.doi.org/10.1021/mz400502v | ACS Macro Lett. 2014, 3, 35−39

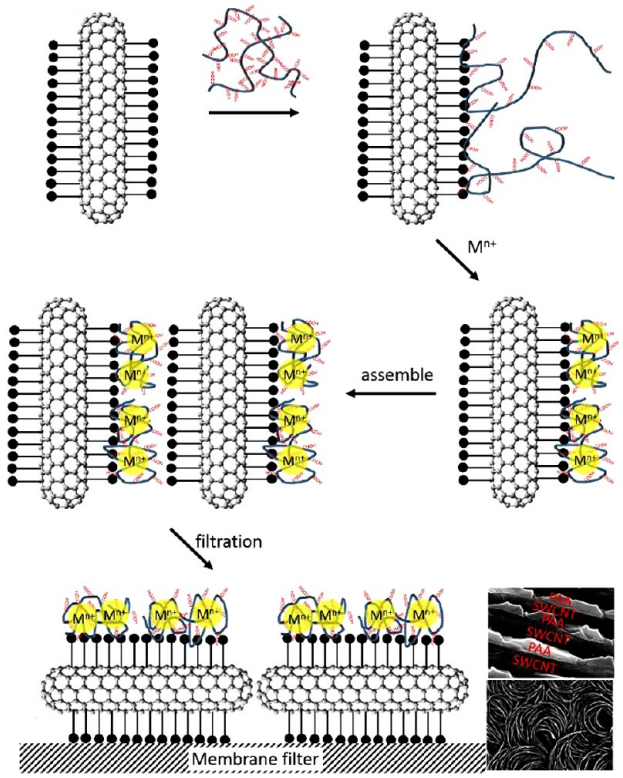

Figure 6. Schematic representation for the formation of ordered PAA microstructures on SWCNT thin film.

SWCNTs. In this study, a great amount of surfactant, SDS, existed in the dispersion system because SWCNTs were predispersed in surfactant solution before they were mixed with polymer solution. Previous research reported that surfactant greatly affects the phase separation behavior in the polymer solution.[40,41] It has also been reported that surfactants formed nanostructural complexes when surfactant molecules were bound to the polymer.[42−44] However, in the controlled experiment we found that the mixture of SDS and PAA derivatives could not produce phase separation and formed ordered microstructures of PAA self-assembly when filtrating on the membrane filter (Supporting Information, Figure S5). Furthermore, when we filtrated the mixture of SDS and PAA onto a separately pre-prepared SWCNT thin film on a membrane filter, ordered PAA self-assembly microstructures also were not observed on SWCNT thin film (Supporting Information, Figure S6). The controlled experiments indicate that SWCNT is of importance for the phase separation and formation of self-assembly microstructures.

Temperature plays an important role in a common phase separation of polymers.[45−47] In our study, the temperature effect was also examined (Supporting Information, Figure S7). After aged at 0 °C, PAA−NH_4 formed domain-like self-assembly on SWCNT thin films rather than the ordered microstructures at room temperature. When the mixture dispersion was aged at 80 °C, blocks or small pieces of microstructures of PAA were formed on the SWCNT thin film. The physical properties such as viscoelasticity of PAA aqueous system are generally temperature-sensitive.[48] Hence, the different microstructures of PAA−NH_4 may originate from the temperature-dependent phase behavior of polymers.

We evaluated the electric conductivity of the microstructures of PAA derivatives on SWCNT thin film. The Ag electrode was used to measure the electric conductivity of PAA thin film. The thickness of PAA thin films was determined by SEM observation (Supporting Information, Figure S8). The apparent $I-V$ response curves of PAA thin films were shown in Figure S9 (Supporting Information). The electric conductivity σ is defined as

$$\sigma = 1/\rho = 1/R{\cdot}L/S \quad (1)$$

where ρ is resistivity; L is the distance between two Ag electrodes; and S is the cross-sectional area of the PAA thin film.

Table 1 summarizes the electric conductivity of three kinds of PAA thin films. Because a large amount of SDS was added in the mixed dispersion system and covered on the surface of SWCNTs, the electric conductivity of the thin film was dramatically influenced by SDS.[49] SWCNT thin films covered by SDS had a conductivity of 0.63 S/cm, a value much lower than that of pure SWCNTs. If PAA phase separated on SWCNT thin films, the conductivity of the system increased to 1.03 S/cm, which was about 2-fold higher than that of SWCNT thin film. As a comparison, SWCNT−SDS−PAA thin film (on mica substrate) shows an electric conductivity as small as 0.042 S/cm, which due to SDS molecules was exceeded in the thin film because they all deposited on mica substrate.

Table 1. $I-V$ Measurement of Various Thin Films Composed of SWCNTs and PAA−NH_4

sample	length (cm)	width (cm)	height (μm)	R (KΩ)	σ (S/cm)
PAA on CNT	0.88	1.0	3.8	2.25	1.03
CNT	0.72	1.0	3.8	3.0	0.63
CNT-PAA on mica	1.0	1.6	160	0.94	0.042

In summary, the phase separation behavior and patterning of PAA derivatives were investigated on SWCNT thin film supported by a membrane filter. PAA salt, including ammonium salt and metal salts such as Na^+, Ag^+, Cu^{2+}, and Fe^{3+}, form ordered microstructures of PAA self-assembly from liquid−liquid phase separation, while PAA−H cannot form any self-assembly structure on the substrate. The morphology of PAA derivative self-assembly is greatly affected by the procedure of pretreatment in the presence of SWCNTs. PAA derivative self-assembly is devoted to the electric conductivity of SWCNT thin films, allowing the use for electric materials. This study improves our knowledge on polymer phase separation on various substrates and suggests an effective approach for formation of SWCNT-based heterogeneous nano-/microstructures.

■ ASSOCIATED CONTENT

Ⓢ Supporting Information

Experiment details and supplemental figures. This material is available free of charge via the Internet at http://pubs.acs.org.

■ AUTHOR INFORMATION

Corresponding Author

*E-mail: zq-tan@jwri.osaka-u.ac.jp.

Notes

The authors declare no competing financial interest.

■ ACKNOWLEDGMENTS

We thank the Ministry of Education, Culture, Sports, Science and Technology of Japan for financial support of this research.

■ REFERENCES

(1) Coleman, J. N.; Khan, U.; Gun'ko, Y. K. *Adv. Mater.* **2006**, *18*, 689−706.
(2) Vigolo, B.; Pénicaud, A.; Coulon, C.; Sauder, C.; Pailler, R.; Journet, C.; Bernier, P.; Poulin, P. *Science* **2008**, *290*, 1331−1334.
(3) lau, K. K. S.; Bico, J.; Teo, K. B. K.; Chhowalla, M.; Amratunga, G. A. J.; Milne, W. I.; Mckinley, G. H.; Gleason, K. K. *Nano Lett.* **2003**, *3*, 1701−1705.
(4) Snow, E. S.; Perkins, F. K.; Houser, E. J.; Badescu, S. C.; Reinecke, T. L. *Science* **2005**, *307*, 1942−1945.
(5) Sekitani, T.; Nakajima, H.; Maeda, H.; Fukushima, T.; Aida, T.; Hata, K.; Someya, T. *Nat. Mater.* **2009**, *8*, 494−499.
(6) Shim, M.; Kam, N. W. S.; Chen, R. J.; Li, Y.; Dai, H. *Nano Lett.* **2002**, *2*, 285−288.
(7) Mamedov, A. A.; Kotov, N. A.; Prato, M.; Guldi, D. M.; Wicksted, J. P.; Hirsch, A. *Nat. Mater.* **2002**, *1*, 190−194.
(8) Li, L.; Li, C. Y.; Ni, C. *J. Am. Chem. Soc.* **2006**, *128*, 1692−1699.
(9) Li, B.; Li, L.; Wang, B.; Li, C. Y. *Nat. Nanotechnol.* **2009**, *4*, 358−362.
(10) Laird, E. D.; Li, C. Y. *Macromolecules* **2013**, *46*, 2877−2891.
(11) Song, M.; Marcolli, C.; Krieger, U. K.; Zuend, A.; Peter, T. *Atmos. Chem. Phys.* **2012**, *12*, 2691−2712.
(12) Arnold, T.; Linke, D. *BioTechniques* **2007**, *43*, 427−440.
(13) Wauquire, J.-P. *Petroleum Refining: separation processes 2*; OPHRYS: Paris, 2000.
(14) Nephew, J. B.; Nihei, T. C.; Carter, S. A. *Phys. Rev. Lett.* **1998**, *80*, 3276−3279.
(15) Chen, Z.-R.; Kornfield, J. A.; Smith, S. D.; Grothaus, J. T.; Satkowski, M. M. *Science* **1997**, *277*, 1248−1253.
(16) De Rosa, C.; Park, C.; Thomas, E. L.; Lotz, B. *Nature* **2000**, *405*, 433−437.
(17) Park, J. W.; Thomas, E. L. *Adv. Mater.* **2003**, *15*, 585−588.
(18) Lopes, W. A.; Jaeger, H. M. *Nature* **2001**, *414*, 735−738.
(19) Thurn-Albrecht, T.; Schotter, J.; Kastle, G. A.; Emley, N.; Shibauchi, T.; Krusin-Elbaum, L.; Guarini, K.; Black, C. T.; Tuominen, M. T.; Russel, T. P. *Science* **2000**, *290*, 2126−2129.
(20) Dufresne, E. R.; Noh, H.; Saranathan, V.; Mochrie, S. G. J.; Cao, H.; Prum, R. O. *Soft Matter* **2009**, *5*, 1792−1795.
(21) Wendlandt, M.; Kerle, T.; Heuberger, M.; Klein, J. *J. Polym. Sci., Part B: Polym. Phys.* **2000**, *38*, 831−837.
(22) Andrew, P.; Huck, W. T. S. *Soft Matter* **2007**, *3*, 230−237.
(23) O'Reilly, R. K.; Hawker, C. J.; Wooley, K. L. *Chem. Soc. Rev.* **2006**, *35*, 1068−1083.
(24) Tanaka, N.; Hirata, G.; Utsumi, I. *Chem. Pharm. Bull.* **1966**, *14*, 414−419.
(25) Zhang, L.; Shen, H.; Eisenberg, A. *Macromolecules* **1997**, *30*, 1001−1011.
(26) Matsuoka, H.; Suetomi, Y.; Kaewsaiha, P.; Matsumoto, K. *Langmuir* **2009**, *25*, 13752−13762.
(27) Irie, M.; Misumi, Y.; Tanaka, T. *Polymer* **1993**, *34*, 4531−4535.
(28) Izutsu, K.-I.; Aoyagi, N.; Kojima, S. *J. Pharm. Sci.* **2005**, *94*, 709−717.
(29) Rivas, B. L.; Pereira, E. D.; Moreno-Villoslada, I. *Prog. Polym. Sci.* **2003**, *28*, 173−208.
(30) Miller, M. L.; O'Donnell, K.; Skogman, J. *J. Colloid Sci.* **1962**, *17*, 649−659.
(31) Leitch, J. J.; Collins, j.; Friedrich, A. K.; Stimming, U.; Dutcher, J. R.; Lipkowski, J. *Langmuir* **2012**, *28*, 2455−2464.
(32) Kavitha, A. L.; Vasudevan, T.; Prabu, H. G. *Desalination* **2011**, *268*, 38−45.
(33) Hu, H.; Saniger, J. M.; Banŭelos, J. G. *Thin Solid Films* **1999**, *347*, 241−247.
(34) Wanless, E. J.; Ducker, W. A. *J. Phys. Chem.* **1996**, *100*, 3207−3214.
(35) Richard, C.; Balavoine, F.; Schultz, P.; Ebbesen, T. W.; Mioskowski, C. *Science* **2003**, *300*, 775−778.
(36) Tan, Z.; Abe, H.; Naito, M.; Ohara, S. *Chem. Commun.* **2010**, *46*, 4363−4365.
(37) Tsai, H.; Lin, J.; Maryani, F.; Huang, C.; Imae, T. *Int. J. Nanomed.* **2013**, *8*, 4427−4440.
(38) Wang, H.; Hobbie, E. K. *Langmuir* **2003**, *19*, 3091−3093.
(39) Wang, W.; Laird, E. D.; Gogotsi, Y.; Li, C. Y. *Carbon* **2012**, *50*, 1769−1775.
(40) Hansson, P.; Lindman, B. *Curr. Opin. Colloid Interface Sci.* **1996**, *1*, 604−613.
(41) Currie, E. P. K.; Stuart, M. A. C.; Borisov, O. V. *Europhys. Lett.* **2000**, *49*, 438−444.
(42) Dubin, P. L.; Oteri, R. *J. Colloid Interface Sci.* **1983**, *95*, 453−461.
(43) Nizri, G.; Magdassi, S.; Schmidt, J.; Cohen, Y.; Talmon, Y. *Langmuir* **2004**, *20*, 4380−4385.
(44) Nizri, G.; Makarsky, A.; Magdassi, S.; Talmon, Y. *Langmuir* **2009**, *25*, 1980−1985.
(45) Kumaki, J.; Hashimoto, T.; Granick, S. *Phys. Rev. Lett.* **1996**, *77*, 1990−1993.
(46) Seuring, J.; Agarwal, S. *Macromol. Rapid Commun.* **2012**, *33*, 1898−1920.
(47) Zhou, X.; Huang, Y. *J. Polym. Sci., Part B: Polym. Phys.* **2002**, *40*, 1334−1341.
(48) Litmanovich, E. A.; Zakharchenko, S. O.; Stoychev, G. V.; Zezin, A. B. *Polym. Sci., Ser. A* **2009**, *51*, 616−621.
(49) Tan, Z.; Ohara, S.; Abe, H.; Naito, M. *Adv. Mater.* **2011**, *23*, 4053−4057.